# Lead isotopic composition and lead source of the Tongchanghe basalt-type native copper-chalcocite deposit in Ninglang, western Yunnan, China*

ZHANG Qian (张 乾)**, ZHU Xiaoqing (朱笑青), and ZHANG Zhengwei (张正伟)
*The Key Laboratory of Ore Deposit Geochemistry, Institute of Geochemistry, Chinese Academy of Sciences, Guiyang 550002, China*

**Abstract** The Tongchanghe native copper-chalcocite deposit at Ninglang occurs in low-Ti basalts of western Yunnan, and the mode of fault-filling & metasomatism metallogenesis indicates that this deposit is of late-stage hydrothermal origin. This makes it more complicated to define the source of ore-forming materials. This paper introduces the Pb isotope data of Himalayan alkali-rich porphyries, regional Early-Middle Proterozoic metamorphic rock basement and various types of rocks of the mining district in western Yunnan with an attempt to constrain the origin of the Tongchanghe native copper-chalcocite deposit at Ninglang. The results showed that the ores are relatively homogeneous in Pb isotopic composition, implying a simple ore-forming material source. The three sets of Pb isotopic ratios in the Himalayan alkali-rich porphyries are all higher than those of the ores; the regional basement metamorphic rocks show a wide range of variations in Pb isotopic ratio, quite different from the isotopic composition of ore lead; the Pb isotopic composition of the Triassic sedimentary rocks and mudstone and siltstone interbeds in the Late Permian Heinishao Formation (corresponding to the forth cycle of basaltic eruption) in the mining district has the characteristics of radiogenic lead and is significantly different from the isotopic composition of ore lead; like the ores, the Emeishan basalts in the mining district and those regionally distributed possess the same Pb isotopic composition, showing a complete overlap with respect to their distribution range. From the above, the possibilities can be ruled out that the ore-forming materials of the Tongchanghe deposit were derived from the basement, a variety of Himalayan magmatic activities, etc. It is thereby defined that the ore-forming materials were derived largely from the Emeishan basalts. From the data available it is deduced that the native cupper-chalcocite-type metallogenesis that occurred in the Emeishan basalt-distributed area has the same metal source as the Tongchanghe deposit.

**Key words** native copper-chalcocite deposit; basalt; Pb isotopic composition; ore-forming material source; Tongchanghe; Yunnan

## 1 Introduction

The native copper-chalcocite deposits associated with the Emeishan basalt have attracted great attention of many scientists engaged in ore deposits in recent years, but their focus is more put on the deposits hosted in the high-Ti basalt area at the boundary of Yunnan and Guizhou (Zhu Bingquan et al., 2002; Liu Yuanhui et al., 2003; Zhu Bingquan, 2003; Zhu Bingquan et al., 2003; Wang Yangeng and Wang Shangyan, 2003; Li Houmin et al., 2004a, b; Zhang Zhengwei et al., 2004). In ore prospecting no breakthrough has yet been made up to now, and only a batch of small-sized mineralization occurrences have been found, for example, the Tongchanghe deposit with a copper reserve of 1643 tons, the Heishanpo occurrence with a copper reserve of 229 tons and the Damingcao occurrence with a copper reserve of 206 tons (Dai Chuangu et al., 2004) within the bounds of Guizhou Province. Around the Dali-Lijiang area of western Yunnan are distributed low-Ti basalts in which are hosted quite a number of native copper-chalcocite assemblage deposits or occurrences, for example, the Tongchanghe, the Zhanhe, the Lamagu, the Mili, the Baoping, the Jin'an, etc. (Qin Dexian et al., 1999; Hu Shouquan et al., 2001), of which the Tongchanghe deposit possesses much better ore-forming conditions and it may be the most typical and largest deposit of its kind (> 100000 t). Unfortunately, it has been less documented. The Tongchanghe deposit occurred in the Emeishan basalt and mudstones, its orebodies are controlled structurally by faults. The basement metamorphic rocks, basalts and the Himalayan magmatic activities have all probably provided ore-forming materials to this deposit. In this work the Pb isotopic composition is

ISSN 1000-9426

* This study was financially supported by the Key Research Orientation Project of Chinese Academy of Sciences (KZCX3-SW-125).

** Corresponding author: zhqiangeol@163.com

used to affirm or repudiate these possibilities.

## 2 Geology

The Tongchanghe deposit is located at the Tongchanghe Village 4.5 km southeast of Ninglang County, western Yunnan. This region just falls within the low-Ti basalt area defined by Xu et al. (2001) and Xiao Long et al. (2003) (Fig. 1). So, merely as viewed from the geological distribution of the deposit (occurrences), the formation of native copper-chalcocite-type deposits has nothing, at least in petrology, to do with the contents of titanium in the basalts, because there is distributed such a type of ore occurrences either in the high-Ti basalt area or in the low-Ti basalt area.

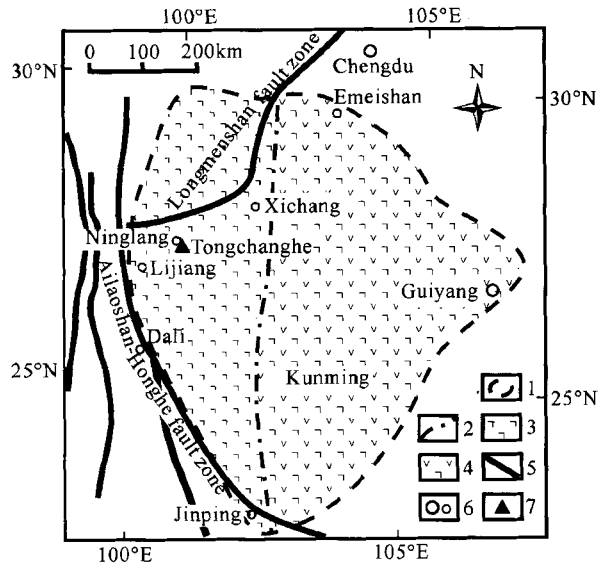


Fig. 1. Sketch showing the geographical position of the Tongchanghe deposit. 1. Distribution area of Emeishan basalts; 2. boundary between high-Ti and low-Ti basalts; 3. distribution area of low-Ti basalts; 4. distribution area of high-Ti basalts; 5. fault zone; 6. residential quarter; 7. Tongchanghe deposit.

### 2.1 Geological background of metallogenesis

The strata exposed in the Tongchanghe mining district are dominated by the Upper Permian Heinishao Formation ($P_2h$) and the third member of the Emeishan basalt ($P_2\beta^3$); in the periphery of the mining district are exposed the Triassic and Upper Devonian strata.

In the western part of the mining district are exposed the Triassic strata, showing a pseudo-conformable relationship with the underlying Permian strata, with alteration seen locally, but mineralization there is of no economic value. The Upper Triassic Songgui Formation ($T_3sg$) consists of grayish-black shales, siltstones and argillaceous sandstones; the Zhongwo Formation ($T_3z$) consists of grey, light grey thick-bedded limestones, with shell limestones at the top; the Middle Triassic Beiya Formation ($T_2b$) consists of limestones interbedded with sandstones in the upper part and of purple sandstones interbedded with yellowish-green shales; the Lower Triassic Lamei Formation ($T_1l$) consists of mudstone, siltstone, feldspathic sandstone, and glauconite sandstone intercalated with minor limestone, with alteration seen locally.

The Permian strata are mainly the Upper Permian Heinishao Formation ($P_2h$) and the third member of the basalt formation ($P_2\beta^3$), the former consisting mainly of amygdaloidal basalt, compact massive basalt intercalated with mottled mudstone, siltstone, basaltic conglomerate, tuff and coal seams, the latter consisting of dark grey porphyrytic basalt, compact massive basalt, and amygdaloidal basalt intercalated with minor tuff.

The Devonian strata are dominated by the Upper Devonian Gangou Formation, composed chiefly of limestone and dolomite, showing an unconformable relationship, or in fault contact, with the overlying Permian strata. No sign of mineralization has been recognized.

Most widespread in the mining district and most closely associated with mineralization are the basalts, which are the product of basic magma eruption in the Emeishan volcano-metallogenic province, almost all copper orebodies are hosted in the basalts (Fig. 2). In the region of western Yunnan the eruption of Emeishan basalts can be divided into four cycles. The forth cycle is represented by the Heinishao Formation, which is also called the upper basalt formation, with copper contents ranging from $80 \times 10^{-6}$ to $380 \times 10^{-6}$. In western Yunnan 55% of native copper-chalcocite mineralization occurs in this stratum. In the mining district the third member of the basalt formation belongs to the third eruption cycle in which there is no or minor sedimentary interbed, indicating the product of magmatic eruption at the peak stage. Its Cu contents are as high as to be $30 \times 10^{-6} - 240 \times 10^{-6}$, in the cycle there is hosted more than 40% of native copper-chalcocite mineralization regionally.

### 2.2 Characteristics of ore-controlling structures

Well developed in the mining district are fault structures, mainly extending south-northwards, northeastwards, north-westwards and east-westwards. The N-E extending faults cut through the other groups of faults, the N-W extending faults cut through the S-N and E-W extending faults, the S-N extending faults cut

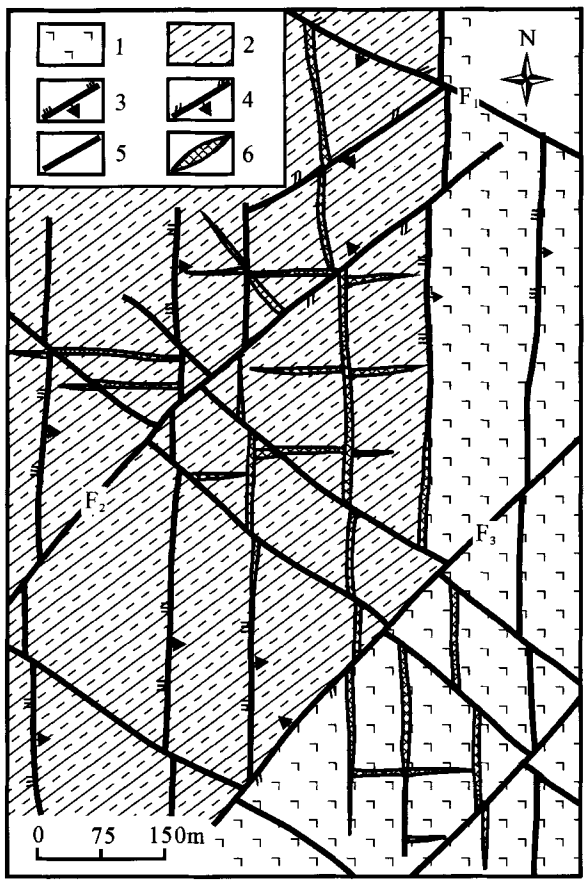


Fig. 2. Geological sketch map of the Tongchanghe deposit. 1. Massive Basalt in the third member of the Late Permian basalt Formation ($P_2\beta^3$); 2. Late Permian Heinishao Formation amygladoidal basalt, massive basalt, shale and siltstone; 3. reversed fault; 4. compresso-shear fault; 5. fault of unknown character; 6. orebody.

through the E-W extending faults. As viewed from the cutting relationships and the patterns of broken orebodies, both N-W and N-E extending faults appear to have formed during the post-ore period, or are fault structures characterized by multi-episodic activities. Mechanically, these faults are dominated by compresso-shear ones, containing almost no ore.

The S-N and E-W extending faults are the major ore-controlling structures in the mining district. The S-N extending faults are large in scale and stably extend, with compressive characteristics. So these faults are the stem ore-controlling faults, which play a role in conduiting and hosting ores. The maim orebodies hosted in the faults are so long as to be over 1500 m. During the post-ore period this group of faults was transformed into compresso-shear ones, thus leading to sliding and deformation of the orebodies on a large scale.

The E-W extending faults are relatively small in scale. Geological field observation led us to see that the faults showed compressive characteristics during the pre-ore period, while they showed tensional characteristics during the ore-forming period with the activities of the S-N extending structures, they, together with the S-N extending faults, were filled and metasomatized by ore fluids, forming veins passing through the S-N extending structures, cross veins and lenticular orebodies (Fig. 2).

### 2.3 Mineralization characteristics

As shown in Fig. 2, orebodies in the Tongchanghe deposit are veined and lenticular in shape. At the time when mineralization occurred at the intersection of the S-N and E-W extending faults, cross-shaped orebodies were usually formed, of the main orebodies the largest one extends so long as to be up to 1500 m, generally within the range of 100 – 300 m. The orebodies extend as deeply as to be over 300 m, copper mineralization is dominant, and the major metal minerals are chalcocite and native copper with minor chalcopyrite and bornite. In the upper oxidation zone one can see covellite, malachite, cuprite, specularite, etc. Nonmetal minerals are mainly epidote, chlorite, quartz, calcite and albite. The corresponding wall-rock alterations are silicification, carbonation, chloritization and epidotization. Ore textures include anhedral-subhedral-euhedral granular texture, metasomatic-resorption texture, metasomatic-relict texture and crush texture; in the near-surface oxidation zone one can see colloidal texture commonly. Ore structures include veined-stockwork structure, veinlet structure, brecciaed structure, crumb structure, disseminated structure, massive structure, crusty structure, etc.

According to alterations and the timing of formation of minerals, four mineralization stages can be distinguished, i. e., (1) calcite-chalcocite metallogenesis stage (I): formation of calcite and scattered chalcocite veinlets, usually cut by veins formed during later stages of mineralization; (2) quartz-epidote-albite-chalcocite metallogenesis stage (II): the main metallogenesis stage, mostly occurring in the middle and lower parts of orebodies and metal minerals occurring largely as being veinlet and massive in quartz veins or quartz-epidote veins, sometimes seen filling in brecciaed ores formed between ores and breccias during stage I; (3) epidote-native copper metallogenesis stage (III): dominant formation of native copper-epidote-type ores, native copper occurring as being mottled, veinlet and crumby while epidote usually occurring as bright green euhedral crystals, which, together with metal minerals, form veinlets cutting through the products of stages (II) and (III) or replacing earlier minerals; (4) hypergenic oxidization stage (IV): surface oxidization zone, generally extending as deeply as 5 – 30 m,

where malachite, azurite and cuprite were formed mainly during this stage. As what is exposed on the Earth's surface is mainly the alteration zone at the tope or in the upper part of orebody, the secondary enrichment of copper is not so remarkable. This indicates that the main orebody of this deposit has not suffered serious denudation, so it possesses bright ore-search perspectives.

In addition, there exists scattered native copper mineralization in the whole basalt in the mining district or in the region studied. Unfortunately the scattered copper mineralization is of no industrial value. According to the results of multi-element analysis of the ore, it is seen that besides copper, local ores also contain higher Au and PGE, but their applicable value needs to be further investigated.

## 3 Samples and analytical methods

As the Tonghechang deposit is controlled tectonically, the basement metamorphic rocks and basalts, as well as Himalayan magmatic activities would be possible to have provided ore-forming materials. So, in addition to ore samples, massive and amygdaloidal basalts, the Heinishao Formation argillaceous rocks and siltstones in the mining district, Triassic Lamei Formation shales and argillaceous siltstones in the periphery of the mining district, we collected 51 samples from the alkali-rich porphyries and regional Early-Middle Proterozoic metamorphic rocks (rock inclusions hosted in the Cangshan metamorphic rocks and alkali-rich porphyries similar in petrological character to the Early-Middle Proterozoic metamorphic rocks) in western Yunnan for Pb isotopic analysis. Meanwhile, we also colleted the Pb isotope data for the Kunyang Group metamorphic rocks (these rocks along with the metamorphic rocks in western Yunnan represent the basement) in central and eastern Yunnan.

**Table 1. The Pb isotopic compositions of the Tongchanghe copper deposit, regional Himalayan alkali-rich porphyries and basement metamorphic rocks**

| Sample No. | Sample locality | Rock or mineral | $^{206}Pb/^{204}Pb$ | $^{207}Pb/^{204}Pb$ | $^{208}Pb/^{204}Pb$ |
|---|---|---|---|---|---|
| JC-19 | Quartz syenite porphyry at Jianchuan | K-feldspar | 18.637 | 15.633 | 38.909 |
| JC-20 | Quartz syenite porphyry at Jianchuan | K-feldspar | 18.595 | 15.662 | 38.874 |
| JC-21 | Quartz syenite porphyry at Jianchuan | K-feldspar | 18.728 | 15.668 | 38.987 |
| LH-31 | Aegirine-augite syenite porphyry at Liuhe | K-feldspar | 18.739 | 15.689 | 38.917 |
| LH-48 | Aegirine-augite syenite porphyry at Liuhe | K-feldspar | 18.718 | 15.687 | 38.900 |
| LH-64 | Aegirine-augite syenite porphyry at Liuhe | K-feldspar | 18.718 | 15.691 | 39.086 |
| SG-6 | Quartz syenite at Songgui | K-feldspar | 18.722 | 15.673 | 39.079 |
| ZH-1 | Syenite porphyry at Zhanhe, Ninglang | K-feldspar | 18.660 | 15.671 | 39.105 |
| SG-4 | Quartz syenite at Songgui | Whole rock | 18.714 | 15.692 | 39.190 |
| SG-7 | Quartz syenite at Songgui | Whole rock | 18.711 | 15.725 | 38.997 |
| LH-34 | Aegirine-augite syenite porphyry at Liuhe | Whole rock | 18.727 | 15.710 | 39.282 |
| ZH-2 | Syenite porphyry at Zhanhe, Ninglang | Whole rock | 18.736 | 15.701 | 39.131 |
| BY-8 | Syenite at Beiya | Whole rock | 18.814 | 15.713 | 39.296 |
| DL-2 | Goutouqing Formation plagioclase amphibolite at Cangshan (Early Proterozoic) | Whole rock | 18.996 | 15.656 | 38.686 |
| DL-4 | Goutouqing Formation plagioclase amphibolite at Cangshan (Early Proterozoic) | Whole rock | 18.491 | 15.630 | 38.660 |
| DL-6 | Goutouqing Formation plagioclase amphibolite at Cangshan (Early Proterozoic) | Whole rock | 18.565 | 15.636 | 38.299 |
| DL-7 | Goutouqing Formation plagioclase amphibolite at Cangshan (Early Proterozoic) | Whole rock | 19.330 | 15.639 | 38.637 |
| XLS-3 | Xuelong Group gneiss (Middle Proterozoic) | Whole rock | 18.911 | 15.718 | 38.409 |
| XLS-6 | Xuelong Group plagioclase-amphibolite (Middle Proterozoic) | Whole rock | 18.639 | 15.679 | 37.939 |
| LH-7 | Muscovite-plagioclase gneiss inclusions in Liuhe rock body | Whole rock | 18.699 | 15.693 | 37.902 |
| LH-26 | Garnet-hornblende schist inclusions in Liuhe rock body | Whole rock | 18.626 | 15.687 | 37.957 |
| JC-2 | Muscovite-alkaline feldspar gneiss inclusions in Jianchuan rock body | Whole rock | 18.603 | 15.690 | 38.561 |
| JC-6 | Muscovite-plagioclase gneiss inclusions in Jianchuan rock body | Whole rock | 8.817 | 15.621 | 38.380 |
| DC-14-3 | Kunyang Group Dayingpan Formation canaceous slate | Whole rock | 18.401 | 15.630 | 38.609 |
| DC-14-5 | Kunyang Group Dayingpan Formation carbonaceous slate | Whole rock | 18.802 | 15.667 | 39.309 |
| YD-11-2 | Kunyang Group Heishan Formation carbonaceous slate | Whole rock | 17.915 | 15.582 | 37.184 |

**Table 1. (To be continued)**

| Sample No. | Sample locality | Rock or mineral | $^{206}Pb/^{204}Pb$ | $^{207}Pb/^{204}Pb$ | $^{208}Pb/^{204}Pb$ |
|---|---|---|---|---|---|
| YD-11-5 | Kunyang Group Heishan Formation carbonaceous slate | Whole rock | 20.221 | 15.715 | 37.256 |
| YD-12-1 | Kunyang Group Heishan Formation carbonaceous slate | Whole rock | 20.043 | 15.790 | 38.078 |
| YD-12-2 | Kunyang Group Heishan Formation carbonaceous slate | Whole rock | 18.698 | 15.608 | 37.178 |
| YD-12-3 | Kunyang Group Heishan Formation carbonaceous slate | Whole rock | 19.549 | 15.708 | 38.816 |
| YD-12-6 | Kunyang Group Heishan Formation carbonaceous slate | Whole rock | 19.333 | 15.706 | 39.457 |
| YD-11-13 | Kunyang Group Luoxue Formation dolomite | Whole rock | 19.018 | 15.649 | 38.227 |
| YD-11-22 | Kunyang Group Luoxue Formation dolomite | Whole rock | 19.858 | 15.732 | 38.363 |
| YD-11-31 | Kunyang Group Luoxue Formation dolomite | Whole rock | 20.993 | 15.850 | 38.160 |
| DC-42-1 | Kunyang Group Caiyuanwan Formation dolomite | Whole rock | 18.522 | 15.655 | 38.137 |
| DC-42-2 | Kunyang Group Caiyuanwan Formation dolomite | Whole rock | 18.334 | 15.667 | 38.166 |
| DC-42-3 | Kunyang Group Caiyuanwan Formation dolomite | Whole rock | 18.334 | 15.626 | 38.011 |
| DC-42-4 | Kunyang Group Caiyuanwan Formation dolomite | Whole rock | 18.539 | 15.659 | 38.162 |
| DC-42-5 | Kunyang Group Caiyuanwan Formation dolomite | Whole rock | 18.357 | 15.689 | 38.182 |
| DC-42-6 | Kunyang Group Caiyuanwan Formation dolomite | Whole rock | 18.855 | 15.657 | 38.345 |
| DC-36-1 | Kunyang Group Sahaigou Formation dolomite | Whole rock | 17.845 | 15.642 | 37.890 |
| DC-36-2 | Kunyang Group Sahaigou Formation dolomite | Whole rock | 17.886 | 15.642 | 38.063 |
| DC-36-3 | Kunyang Group Sahaigou Formation dolomite | Whole rock | 17.781 | 15.633 | 37.763 |
| DC-36-4 | Kunyang Group Sahaigou Formation dolomite | Whole rock | 17.876 | 15.657 | 37.944 |
| DC-36-5 | Kunyang Group Sahaigou Formation dolomite | Whole rock | 17.969 | 15.627 | 38.124 |
| DC-36-6 | Kunyang Group Sahaigou Formation dolomite | Whole rock | 18.151 | 15.689 | 37.924 |
| YD-11-44 | Kunyang Group Yinmin Formation dolomite | Whole rock | 18.959 | 15.657 | 39.342 |
| NT-21 | $P_2\beta^3$ massive basalt | Whole rock | 18.543 | 15.571 | 38.861 |
| NT-22 | $P_2\beta^3$ massive basalt | Whole rock | 18.357 | 15.472 | 38.493 |
| NT-23 | $P_2\beta^3$ massive basalt | Whole rock | 18.403 | 15.552 | 38.722 |
| NT-25 | $P_2\beta^3$ massive basalt | Whole rock | 18.599 | 15.573 | 38.824 |
| NT-26 | $P_2\beta^3$ massive basalt | Whole rock | 18.529 | 15.561 | 39.043 |
| NT-27 | $P_2\beta^3$ massive basalt | Whole rock | 18.503 | 15.507 | 38.642 |
| NT-30 | Heinishao Formation amygdaloidal basalt ($P_2h$) | Whole rock | 18.606 | 15.598 | 38.791 |
| NT-31 | Heinishao Formation amygdaloidal basalt ($P_2h$) | Whole rock | 18.695 | 15.589 | 38.983 |
| NT-32 | Heinishao Formation massive basalt ($P_2h$) | Whole rock | 18.552 | 15.547 | 38.608 |
| NT-33 | Heinishao Formation mudstone ($P_2h$) | Whole rock | 18.909 | 15.704 | 39.414 |
| NT-36 | Heinishao Formation mudstone ($P_2h$) | Whole rock | 19.032 | 15.793 | 39.725 |
| NT-37 | Heinishao Formation siltstone ($P_2h$) | Whole rock | 18.784 | 15.772 | 39.162 |
| NT-40 | Lower Triassic Lamei Formation shale | Whole rock | 18.799 | 15.667 | 38.894 |
| NT-41 | Lower Triassic Lamei Formation shale | Whole rock | 18.897 | 15.741 | 39.011 |
| NT-43 | Lower Triassic Lamei Formation mudstone | Whole rock | 18.816 | 15.729 | 38.902 |
| NT-44 | Lower Triassic Lamei Formation mudstone | Whole rock | 19.152 | 15.839 | 39.226 |
| NT-1 | Mineralization alteration zone in western mining district | Chalcopyrite | 18.502 | 15.569 | 38.614 |
| NT-2 | Mineralization alteration zone in western mining district | Chalcocite | 18.671 | 15.573 | 38.795 |
| NT-4 | Mineralization alteration zone in western mining district | Quartz | 18.378 | 15.561 | 38.881 |
| NT-5 | Mineralization alteration zone in western mining district | Chalcocite | 18.469 | 15.508 | 38.599 |
| NT-9 | Mienralization alteration zone in western mining district | Chalcopyrite | 18.277 | 15.547 | 38.637 |
| NT-12 | Mineralization alteration zone in western mining district | Chalcocite | 18.499 | 15.583 | 38.602 |
| NT-13 | Mineralization alteration zone in western mining district | Chalcopyrite | 18.294 | 15.473 | 38.563 |
| NT-14 | Mineralization alteration zone in eastern mining district | Chalcocite | 18.378 | 15.526 | 38.549 |
| NT-15 | Mineralization alteration zone in eastern mining district | Chalcocite | 18.558 | 15.592 | 38.926 |
| NT-16 | Mineralization alteration zone in eastern mining district | Bornite | 18.589 | 15.519 | 39.001 |
| NT-17 | Mineralization alteration zone in eastern mining district | Quuartz | 18.520 | 15.598 | 38.738 |
| NT-18 | Mineralization alteration zone in eastern mining district | Chalcocite | 18.482 | 15.523 | 38.876 |

Note: The Kunyang Group samples from Chang Xiangyang et al. (2002a, b), DD-X and BZ-X from Zhang Zhaochong and Wang Fusheng (2003), the rest are samples in this study. Analytical errors ($2\sigma$): $^{206}Pb/^{204}Pb < \pm 0.016$, $^{207}Pb/^{204}Pb < \pm 0.010$, $^{208}Pb/^{204}Pb < \pm 0.021$ for whole rocks; $^{206}Pb/^{204}Pb < \pm 0.013$, $^{207}Pb/^{204}Pb < \pm 0.010$, $^{208}Pb/^{204}Pb < \pm 0.019$ for K-feldspar; $^{206}Pb/^{204}Pb < \pm 0.014$, $^{207}Pb/^{204}Pb < \pm 0.012$, $^{208}Pb/^{204}Pb < \pm 0.018$ for sulfides.

0.5 g of quartz, feldspar, basalt, shale and alkali-rich porphyry samples was taken respectively, followed by the addition of 2 – 3 drops of nitric acid and 2 mL concentrated HF, and then was decomposed at low

temperature over 2 – 3 days and nights. Then, several drops of $HClO_4$ were added to completely eliminate the remained HF and $SiF_4$ at high temperature. 0.2 g of chalcocite and bornite samples was weighed and taken respectively, followed by the addition of aqua regia to decompose the samples at low temperature over 2 – 3 days and nights and then evaporated till dryness. The residues of the samples mentioned above were separated on an anion resin exchange column (AG 1 × 8, 200 – 400 mesh) by adopting the HBr system for the sake of Pb extraction and purification, with silica gel as the propellant. The measurement of Pb isotopic composition was effected on a VG354 solid mass spectrometer made in England at the Laboratory of Isotopes of the Institute of Geology and Geophysics, Chinese Academy of Sciences and the results are listed in Table 1. The results of measurement were calibrated using standard sample NBS981; the results of continuous determination showed that the isotope fractionation is better than 0.1% and the overall errors involved in the measurements are less than 3%.

## 4 Discussion

### 4.1 The compositional characteristics of ore lead

The 12 samples for the analysis of their ore lead isotopic composition include chalcocite (7), chalcopyrite (2), bornite (1) and quartz (2), respectively belonging to the products of mineralization at different stages in different locations. As viewed from the results of Pb isotopic analysis (Table 1), it is seen clearly that different minerals all show basic similarities in Pb isotopic composition and vary isotopically over the same range, i. e., $^{206}Pb/^{204}Pb$ between 18.277 – 18.671, $^{207}Pb/^{204}Pb$ between 15.473 – 15.598, and $^{208}Pb/^{204}Pb$ between 38.549 – 39.001. It can be seen that the Pb isotopic ratios vary over a very narrow range (Fig. 3).

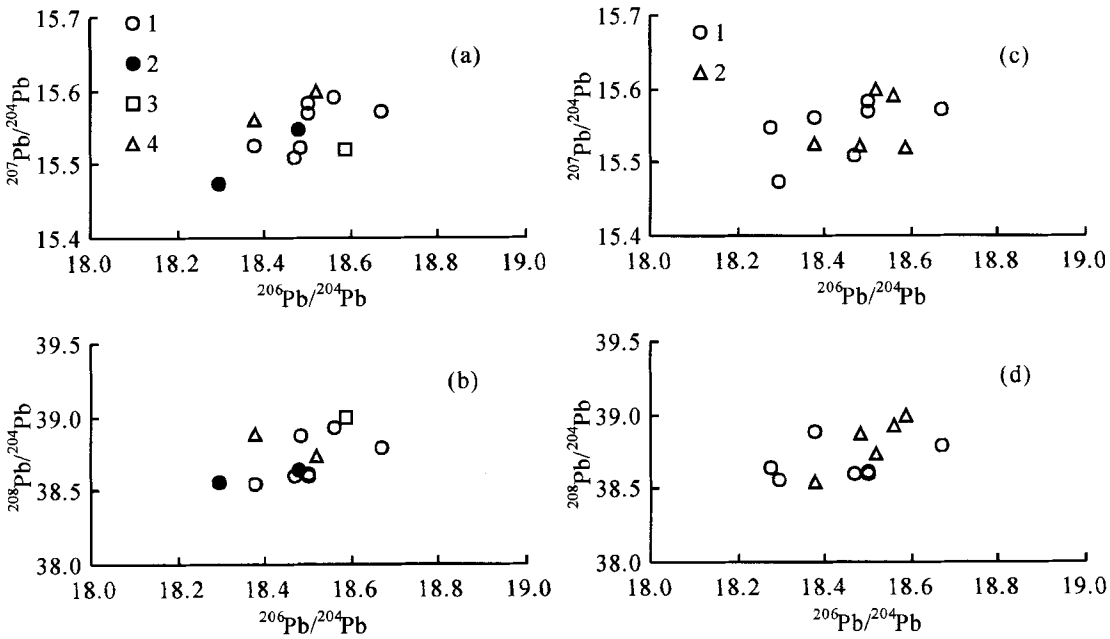


Fig. 3. The isotopic composition of ore lead of the Tongchanghe deposit. (a) and (b). Pb isotopic composition of different minerals: 1. chalcocite; 2. chalcopyrite; 3. bornite; 4. quartz. (c) and (d). Isotopic composition of ore lead in different stages of metallogenesis: 1. Quartz-epidote-albite-chalcocite metallogenesis stage (II); 2. epidote-native copper metallogenesis stage (III).

The identical Pb isotopic composition indicates that lead of different stages in the Tongchanghe deposit has the same source, implying that the major element copper appears to be of single source.

### 4.2 Pb isotopic composition of the regional basement metamorphic rocks and its relationship with ore lead

In the Tongchanghe deposit and its vast vicinity are exposed no metamorphic basement strata. From central to eastern Yunnan are widespread the Kunyang Group-predominated Middle Proterozoic metamorphic rocks, along the marginal parts of the Jinshajiang-Ailaoshan fault zone are distributed the Early-Middle Proterozoic Cangshan and Xuelongshan metamorphic rocks, indicating that there also exists Early-Middle Proterozoic metamorphic basement at depth in the Tongchanghe mining district. Fluids which were cycling at depth may have extracted ore-forming elements from these metamorphic rocks (Zhang Zhenliang et al., 2005). Therefore, we analyzed the Pb isotopic compositions of schist and gneiss samples from the

Goutouqing Formation of the Cangshan Group, the Xuelongshan Group and gneiss xeloliths (corresponding in petrologic character to Middle Proterozoic metamorphic rocks) in the Jianchuan massif, and at the meantime we colleted the analytical results for the Kunshan Group rocks by Chang Xiangyang et al. (2002a, b).

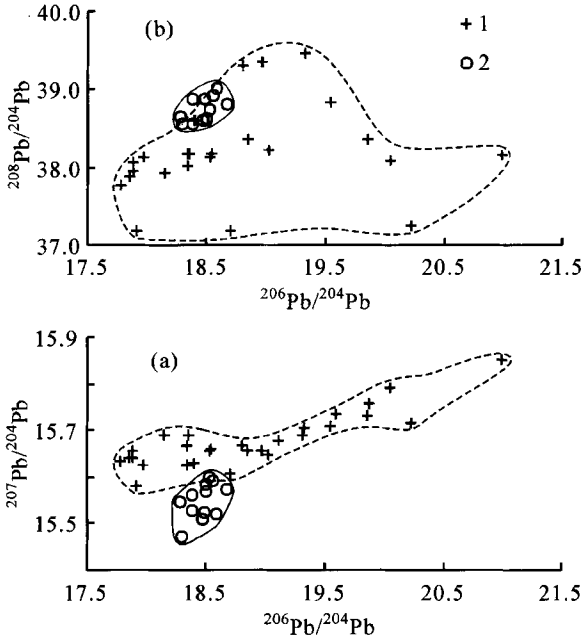


Fig. 4. Comparison of ore lead with lead in the Early-Middle Proterozoic rocks. 1. Lead in Early-Middle Proterozoic rocks; 2. ore lead.

As can be seen from Table 1 and Fig. 4, the regional metamorphic basement is characterized by a wide range of variations in Pb isotopic composition, and various kinds of samples are recognized from relatively low to very high Pb isotopic ratios. For example, $^{206}Pb/^{204}Pb$ ratios may be so high as to reach 21, $^{207}Pb/^{204}Pb$ ratios even up to 15.85, and $^{208}Pb/^{204}Pb$ ratios, to 39.5. As compared with the relatively even isotopic composition of ore lead, the lead in metamorphic rocks belongs to a completely different isotopic evolution system. Such significant differences in Pb isotopic composition between ores and basement rocks indicate that there is no affinity between them. From this deduction the possibility can be ruled out that the old metamorphic rocks at depth in the mining district provided ore-forming materials for the Tongchanghe deposit.

### 4.3 The Pb isotopic composition of the Himalayan alkali-rich magmatic rocks and its relationship with ore lead

The Himalayan alkali-rich porphyries distributed along the Jinshajiang-Ailaoshan fault zone in western Yunnan are closely related with copper sulfide minerogenesis (Bi Xianwu et al., 2000). According to the interpretative data of satellite photos, there would exist a concealed porphyry body at depth in the Tongchanghe ore-mining district, spatially belonging to the Jinshajiang-Ailaoshan Himalayan alkali-rich rock belt (Hu Shouquan et al., 2001). Then, what role the intrusion of this concealed porphyry body played in the formation of the Tongchanghe deposit, especially whether it provided ore-forming materials to the deposit, must a question to be addressed.

According to Liu Xianfan et al. (1999) and Zhang Qian et al. (2002), different alkali-rich porphyry bodies distributed in the region of western Yunnan have consistent Pb isotopic composition. So we analyzed the Pb isotopic composition of feldspar and whole-rock samples from some of the regionally distributed alkali-rich porphyry bodies (Table 1). The analytical results show that although the Pb isotopic composition of the alkali-rich porphyry whole rock is generally slightly higher than that of feldspar, there is no significant difference between the two (Fig. 5). The timing of intrusion of the alkali-rich porphyries in western Yunnan is generally within the range of 15 – 25 Ma. During this short period of time the radiogenic Pb resultant from the decay of U and Th is limited in amount, and this may be the main reason why the whole rock is close to feldspar in Pb isotopic composition.

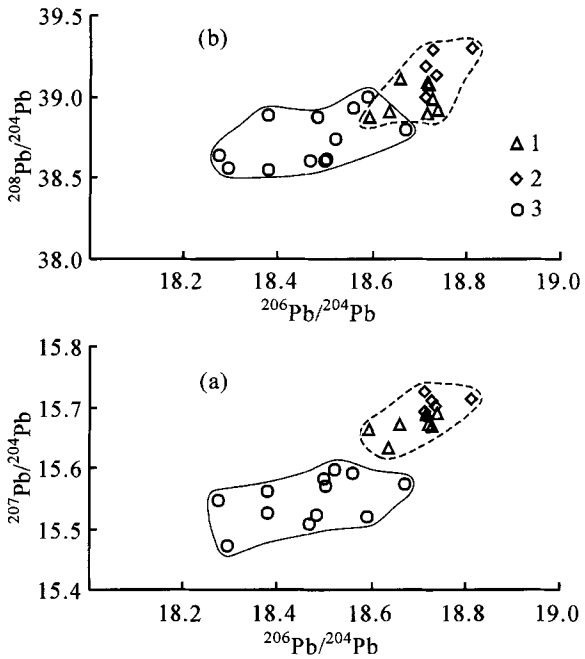


Fig. 5. Comparison of the Pb isotopic composition of ores from the Tongchanghe deposit with that of of the Himalayan alkali-rich porphyries. 1. Alkali-rich whole rock; 2. K-feldspar in the alkali-rich porphyries; 3. ore.

By comparing the Pb isotopic composition of ores from the Tongchanghe deposit with that of the alkali-rich porphyries it can be seen clearly that there is significant difference between the two (Table 1, Fig. 5). On the $^{206}Pb/^{204}Pb$-$^{207}Pb/^{204}Pb$ diagram (Fig. 5a) their respective projecting points fall within the two independent areas, while on the $^{206}Pb/^{204}Pb$-$^{208}Pb/^{204}Pb$

diagram (Fig. 5b), the isotopic ratios of ore lead are generally lower than those of porphyries, though their respective projecting points slightly overlap. From the above it can be said with certainty that such fluids that their Pb isotopic composition is even lower than that of the magma itself could by no means be differentiated from the Himalayan alkali-rich magma. That is to say, the ore-forming materials for the Tongchanghe deposit were not provided by the Himalayan alkali-rich magma.

## 4.4 The Pb isotopic composition of various kinds of ore in the mining district and its relationship with ore lead

### *4.4.1 Lead isotopic composition of Triassic argillaceous rocks and shales*

The Triassic strata exposed in the periphery of the mining district are the cover rocks of the Emeishan basalts, which are composed chiefly of sandstone, argillaceous siltstone, shale and carbonate rock. The Pb isotopic composition (Table 1) of the Lower Triassic Lamei Formation argillaceous rocks and shales collected from the periphery of the western part of the mining district indicates that the lead is obviously of radiogenesis, which has relatively high isotopic ratios, far away from the field of ore lead (Fig. 6).

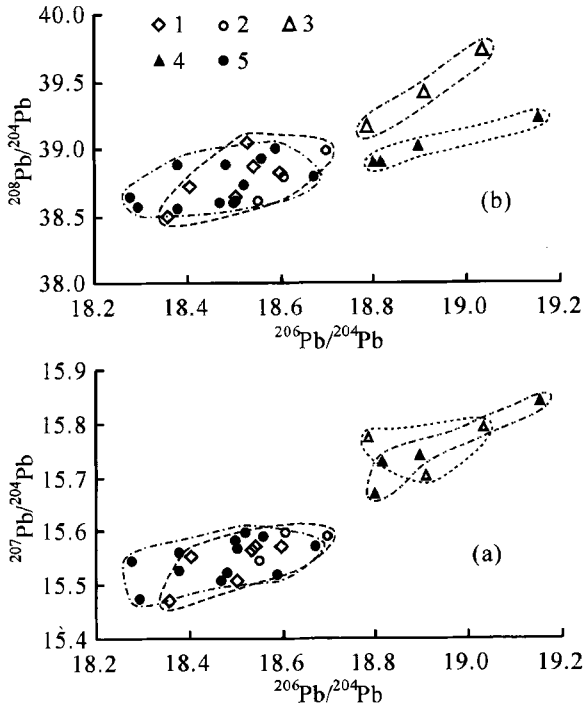


Fig. 6. Pb isotopic composition of various types of rocks in the mining district and their relationships with ore lead. 1. Massive basalt in the third member of the basalt formation; 2. Heinishao Formation amygdaloidal basalt; 3. Heinishao Formation shale; 4. Lower Triassic mudstone; 5. ore.

The Triassic strata provided ore-forming materials for the Tongchanghe deposit, and the most important path is that the strata were leached by downward penetrating fluids. But as viewed from the Pb isotopic composition, the possibility can be completely ruled out that the cover strata provided ore-forming materials because it is impossible to have leached out such ore-forming materials from the rocks that their Pb isotopic composition is still lower than that of the rocks themselves.

### *4.4.2 The Pb isotopic composition of the Heinishao Formation mudstones and siltstones*

The Heinishao Formation siltstones and mudstones are interbedded with basalts and also are the wall rocks of orebodies. The Pb isotopic composition of three samples is also indicative of radiogenesis (Table 1, Fig. 6). In the U-Pb system (Fig. 6a) the samples fall within the area which overlaps that of the Lower Triassic rock samples, indicating that they have the same evolutionary system. But in Fig. 6b it can be seen that the samples are precisely still more enriched in $^{208}Pb$ than the Triassic rocks, providing evidence suggesting that they have different Th-Pb evolutionary systems.

Precisely, being far higher than the isotopic composition of ore lead also indicates that the Heinishao Formation argillaceous rocks did not provide any ore-forming material for the formation of the Tongchanghe deposit.

### *4.4.3 The Pb isotopic composition of basalt and its relationship with ore lead*

Massive basalt in the third member of the basalt formation and basalt in the Heinishao Formation are both the most important wall rocks of orebodies. Nine whole-rock samples were isotopically analyzed to give $^{206}Pb/^{204}Pb$ ratios ranging from 18.357 – 18.695; $^{207}Pb/^{204}Pb$ ratios, 15.472 – 15.598; and $^{208}Pb/^{204}Pb$ ratios, 38.493 – 39.043 (Table 1). This variation trend of Pb isotopic ratios is the same as that of the Lijiang, Yongsheng and Yanyuan basalts in western Yunnan (Zhang Zhaochong and Wang Fusheng, 2003), indicating that basalts distributed in the vast area of western Yunnan have a consistent Pb isotopic composition.

As is shown in Fig. 6, the area within which the Pb isotopic composition of basalts in the mining district falls generally overlaps with the area in which the ore lead is distributed. Due to the lack of definite metallogenesis time of the Tongchanghe deposit, the Pb isotopic composition of basalts can by no means be correlated to that of rocks at the time of metallogenesis. Hu Shouquan et al. (2001) deduced that the formation of this deposit is closely related with the concealed Himalayan magmatism at depth in the mining district, so its metallogenetic age should be designated to the Himalayan (20 – 40 Ma). After the Pb isotopic composition

of basalts was correlated in accordance with this age value, it was found that as the contents of U and Th in the basalts are considerably low [$(1-4)\times10^{-6}$ and $(3-7)\times10^{-6}$, respectively], only a minor amount of radiogenetic lead could be produced from the decay of U and Th in the rocks during the period of 20 – 40 Ma, which hence could not exert an essential influence on the whole-rock Pb isotopic analysis. Such a conclusion can be drawn from Fig. 6 that the ore lead stemmed from the Emeishan basalts. Meanwhile, the ore-hosted fault structures are all pre-ore fault structures and experienced many episodes of tectonic activities (Hu Shouquan et al., 2001). All this indicates that the fault structures occurred after the petrogenesis of basalts. Filling-metasomatic metallogenetic mode indicates that metallogenesis not only postdated the basalts, but also postdated the fault structures.

According to Hu Shouquan et al. (2001), the $\delta^{34}S_{SMOW}$ values of sulfates from the Tongchanghe deposit are −4.9‰ – −9.7‰; the $\delta^{13}C_{PDB}$ and $\delta^{18}O_{SMOW}$ values of calcite are −6.7‰ – −9.0‰ and 13.3‰ – 18.9‰, respectively; the homogenization temperatures of fluid inclusions in quartz and calcite are 115 – 220℃. The H and O isotopic composition of fluid inclusions from two quartz samples was analyzed, yielding $\delta^{18}O_{H_2O}$ values of −3‰ – −7‰ and δD values of −66‰ to −72‰, indicating that ore fluids stemmed from meteoric waters. So the process of formation of this deposit can be briefly described as follows. Heated meteoric waters circulated within plutonic basalts and leached out copper and other ore-forming materials, forming Cu-bearing fluids; under the action of tectonic dynamics the ore-forming fluids migrated upwards into the metallogenetically structural system, followed by the occurrence of filling-metasomatism; under low temperature and relatively oxidizing conditions the Tongchanghe native copper-chalcocite deposit was formed.

## 5 Conclusions

The Tongchanghe native copper-chalcocite deposit occurred in the Emeishan basalts of the third and fourth cycles of the Late Permian and the orebodies are strictly controlled by structures, indicating that the deposit postdated basalt metallogenesis and fault structures.

The Pb isotopic composition of ores is similar to that of the Himalayan alkali-rich porphyries, regional Early-Middle Proterozoic metamorphic rocks, Triassic argillaceous rocks and Late Permian Heinishao Formation siltstones and argillaceous rocks in western Yunnan, implicating that these rocks did not provide any lead for the deposit; both ores and Emeishan basalts have identical Pb isotopic compositions. From this it can be said with certainty that lead in the ore stemmed from the basalts leached by fluids. In the process of leaching copper in the rocks entered into fluids in large amounts to form Cu-bearing hydrothermal solutions, and filling-metasomatism of the solutions along the faults led to the formation of the Tongchanghe deposit.

The widespread of native copper-calcocite deposits associated with the Emeishan basalts in the low-Ti basalt area of western Yunnan indicates that the formation of this type of copper deposits has nothing to do with the type of basalt.

**Acknowledgements** In the geological fieldwork of this research doctor Yang Weiguang and senior engineer Sha Shaoli with the No. 3 Geological Party of Yunnan Province Bureau of Geology and Mineral Resource offered their warm help. Doctor Zhen Xiangshen with the Institute of Geology and Geophysics, Chinese Academy of Sciences, helped accomplish the Pb isotopic analysis and measurement of samples. The authors would like to extend their cordial thanks to them all.

## References

Bi Xianwu, Hu Ruizhong, and Ye Zaojun (2000) Relations between A-type granites and copper mineralization as exemplified by the Machangqing Cu deposit [J]. *Science in China* (Series D), **43**, 93 – 102.

Chang Xiangyang, and Zhu Bingquan (2002a) Isotope geochemistry of the Dongchuan copper deposit, Yunnan, SW China: Stratigraphic chronology and application of lead isotopes in geochemical exploration [J]. *Chinese Journal of Geochemistry*. **21**, 65 – 72.

Chang Xiangyang, Zhu Bingquan, and Mo Xiangyun (2002b) Geochemical studies of sodium enriched metavolcanite series in the area of Longbohe copper deposit, Yunnan Province, SW China: Nd, Sr and Pb isotopic characteristics and chronology [J]. *Chinese Journal of Geochemistry*. **21**, 163 – 169.

Dai Chuangu, Liu Aimin, Wang Ming, and Wu Guangren (2004) Characteristics and mineralization of Emeishan basaltic copper deposits in the west of Guizhou Province [J]. *Guizhou Geology*. **21**, 71 – 75 (in Chinese with English abstract).

Hu Shouquan, Guo Wenping, Yang Fenggen, Xu Zhanzhang, and Zhang Shouting (2001) A study on the metallogenetic condition of Tongchanghe Cu deposit in Ninglang, Yunnan [J]. *Yunnan Geology*. **20**, 46 – 58 (in Chinese with English abstract).

Li Houmin, Mao Jingwen, Xu Zhangbao, Chen Yuchuan, Zhang Changqing, and Xu Hong (2004a) Copper mineralization characteristics of the Emeishan basalt district in the Yunnan-Guizhou border area [J]. *Acta Geoscientica Sinica*. **25**, 495 – 502 (in Chinese with English abstract).

Li Houmin, Mao Jingwen, Zhang Changqing, Xu Hong, Chen Yuchuan, and Wang Denghong (2004b) Isotopic geochemistry of Emeishan basalt copper deposits in northeastern Yunnan and western Guizhou [J]. *Mineral Deposits*. **23**, 232 – 240 (in Chinese with English abstract).

Liu Xianfan, Zhan Xinzhi, Gao Zhenmin, Liu Jiajun, Li Chaoyang, and Su Wenchao (1999) Deep xenoliths in alkalic porphyry, Liuhe, Yunnan, and implications to petrogenesis of alkalic porphyry and associated mineralizations [J]. *Science in China* (Series D). **42**, 627 – 635.

Liu Yuanhui, Li Jin, and Deng Keyong (2003) Geological conditions of copper deposits associated with the Emeishan basalt in the Panxian area, Guizhou [J]. *Geological Bulletin of China*. **22**, 713 – 717 (in Chinese with English abstract).

Qin Dexian, Yan Yongfeng, Lin Youbin, Tian Yulong, and Liu Wei (1999) Basalt along Chenghai fault and its relations to metallization [J]. *Geological Exploration for Non-Ferrous Metals*. **8**, 373 – 377 (in Chinese with English abstract).

Wang Yangeng and Wang Shangyan (2003) Emeishan large igneous provinces and basalt copper deposits: An example from Permian ba-

salt areas in Guizhou [J]. *Guizhou Geology*. **20**, 5 - 10 (in Chinese with English abstract).

Xiao Long, Xu Yigang, and He Bin (2003) Emei mantle plume-subcontinental lithosphere interaction: Sr-Nd and O isotopic evidence from low-Ti and high-Ti basalts [J]. *Geological Journal of China Universities*. **9**, 207 - 217 (in Chinese with English abstract).

Xu Y. G., Chung S. L., Jahn B. M., and Wu G. Y. (2001) Petrologic and geochemical constraints on the petrogenesis of Permian-Triassic Emeishan flood basalts in southwestern China [J]. *Lithos*. **58**, 145 - 168.

Zhang Qian, Pan Jiayong, Liu Jiajun, Shao Shushun, and Liu Zhihao (2002) Determination and application of the upper mantle lead composition in the western Yunnan [J]. *Geology-Geochemistry*. **30**, 1 - 6 (in Chinese with English abstract).

Zhang Zhaochong and Wang Fusheng (2003) Sr, Nd and Pb isotopic characteristics of Emeishan basalt province and discussion on their source region [J]. *Earth Science—Journal of China University of Geosciences*. **28**, 431 - 439 (in Chinese with English abstract).

Zhang Zhengwei, Cheng Zhandong, Zhu Bingquan, Zhang Qian, Zhu Xiaoqing, and Hu Yaoguo (2004) The relationship between the Emeishan basalt formation and copper mineralization [J]. *Acta Geoscientica Sinica*. **25**, 503 - 508 (in Chinese with English abstract).

Zhang Zhenliang, Huang Zhilong, Guan Tao, Yan Zaifei, and Gao Derong (2005) Study on the multi-sources of ore-forming materials and ore-forming fluids in the Huize lead-zinc ore deposit [J]. *Chinese Journal of Geochemistry*. **24**, 243 - 252.

Zhu Bingquan (2003) Continental flood basalts and copper deposits of the Keweenawan type [J]. *Geology-Geochemistry*. **31**, 1 - 8 (in Chinese with English abstract).

Zhu Bingquan, Chang Xiangyang, Hu Yaoguo, and Zhang Zhengwei (2002) Discovery of Yanhe copper deposit in the Yunnan-Guizhou border area and a new train of thought for copper prospecting in the large igneous province of Emeishan flood basalts [J]. *Advance in Earth Sciences*. **17**, 912 - 917 (in Chinese with English abstract).

Zhu Bingquan, Hu Yaoguo, Zhang Zhengwei, and Chang Xiangyang (2003) Discovery of the copper deposits with features of the Keweenawan type in the border area of Yunnan and Guizhou provinces [J]. *Science in China* (Series D). **6** (supp.), 60 - 72.